

Mass transport of alkali metal with pulses in a surface reaction

Liu Hong,¹ H. Uecker,² M. Hinz,¹ L. Qiao,³ I. G. Kevrekidis,³ S. Günther,⁴ T. O. Mendes,⁵ A. Locatelli,⁵ and R. Imbihl^{1,*}

¹*Institut für Physikalische Chemie und Elektrochemie, Leibniz-Universität Hannover, Callinstrasse 3-3a, D-30167 Hannover, Germany*

²*Institut für Mathematik, Carl von Ossietzky Universität Oldenburg, D-26111 Oldenburg, Germany*

³*Department of Chemical Engineering, Princeton University, Princeton, New Jersey 08544, USA*

⁴*Department of Chemistry, Universität München, Butenandtstr. 5-13 E, 81377 München, Germany*

⁵*Sincrotrone Trieste, Area Science Park-Basovizza, I-34012 Trieste, Italy*

(Received 14 December 2007; revised manuscript received 16 May 2008; published 20 November 2008)

It is shown that the pulses which develop in the NO+H₂ reaction on an alkali promoted Rh(110) surface reaction can transport alkali metal. This leads to the accumulation of a substantial alkali-metal concentration in the collision area of pulse trains. Realistic simulations revealed that the effect is due to the strong energetic interactions of the alkali metal with coadsorbates, i.e., the attractive interaction with coadsorbed oxygen and the effectively repulsive interaction with coadsorbed nitrogen.

DOI: [10.1103/PhysRevE.78.055203](https://doi.org/10.1103/PhysRevE.78.055203)

PACS number(s): 82.40.Bj, 82.65.+r

Under conditions far from thermodynamical equilibrium chemical reaction diffusion (RD) systems may exhibit spatiotemporal patterns such as simple reaction fronts, rotating spiral waves, or stationary concentration (Turing) patterns [1]. These patterns arise due to the coupling of diffusion with a nonlinear reaction. If, in addition, energetic interactions between the reacting particles are present these interactions may enforce the formation of separate domains of the reactants (“reactive phase separation”) [2–4]. For example, the coupling of a reaction with phase separating polymer mixtures or two-component Langmuir layers was shown to induce chemical wave patterns [5,6]. On surfaces energetic interactions between adsorbed particles are practically always present as is well known from the observation of two-dimensional ordered adlayers. The stationary concentration patterns seen in the O₂+H₂ reaction on a Rh(110) surface predosed with some potassium were shown to be caused by the strong chemical affinity between potassium and coadsorbed oxygen [4,7]. Similarly, on a Rh(110) surface alloyed with atomically thin layers of Au and Pd a phase separation into Rh(110)/O and Pd/Au was observed in the O₂+H₂ reaction [8]. Monte Carlo simulations of promoters and poisons on catalytic surfaces with attractive interactions have been conducted showing traveling islands [9].

In this Rapid Communication we report on an effect which also relies on the strong chemical interaction of an alkali promoter with other adsorbates, namely, the transport of the promoter species with pulses in an excitable surface reaction. We study the NO+H₂ reaction on a Rh(110) surface covered with a submonolayer coverage of potassium [10]. The unpromoted system Rh(110)/NO+H₂ exhibits a variety of chemical wave patterns ranging from elliptically and rectangularly shaped target patterns to traveling wave fragments [11,12]. With low to medium potassium coverages the system retains its excitability but we observe that the initially homogeneously distributed K is transported by traveling pulses across the surface. The experiments are comple-

mented by simulations with a realistic model which incorporates as an essential element the non-Fickian diffusion of potassium.

For following the reaction dynamics we use photoemission electron microscopy (PEEM) which utilizes photons from a D₂ discharge lamp (5.5–6 eV) to image the local work function (WF) with a resolution of $\approx 1 \mu\text{m}$. A chemical identification of the adspecies was obtained by spectroscopic photoemission and low energy electron microscopy (SPELEEM), a synchrotron-based energy-filtered PEEM which allows microspot x-ray photoelectron spectroscopy (XPS) measurements [13]. Potassium was deposited with a getter source (SAES) and the K coverage was determined with Auger electron spectroscopy and by identification of the K-induced reconstruction phases in low-energy electron diffraction (LEED) [14]. Both gases, NO and H₂, adsorb dissociatively on the Rh(110) surface and the dissociation products recombine on the surface to form the product molecules N₂ and H₂O which rapidly desorb.

Starting with a homogeneously K covered surface with $\theta_{\text{K}}^{\text{init}}=0.06\text{ML}$ (monolayer) the introduction of the two gases, NO+H₂, leads to the formation of target patterns. The PEEM images in Fig. 1(a) display two pulse trains which collide about in the middle of the imaged area. The traveling white bands represent a nitrogen covered surface, whereas oxygen which strongly increases the WF appears as a dark area. One observes that a bright zone forms in the collision area of the pulses whose brightness and lateral extension increase with each subsequent pulse collision. Figure 1(b) displays the local brightness in the collision area and the PEEM intensity integrated over the central area.

The formation of a very bright area has to be assigned to potassium, which is known to strongly lower the WF of the metal surface by as much as 4 eV [15]. Since the integrated brightness grows with each colliding pair of pulses potassium is apparently transported by traveling pulses. The enrichment process continues only for a limited time (0.5–1 h) because the system becomes progressively disordered until finally well-defined pulse trains no longer exist. From calibration of the PEEM brightness with a known amount of

*Corresponding author; imbihl@pci.uni-hannover.de

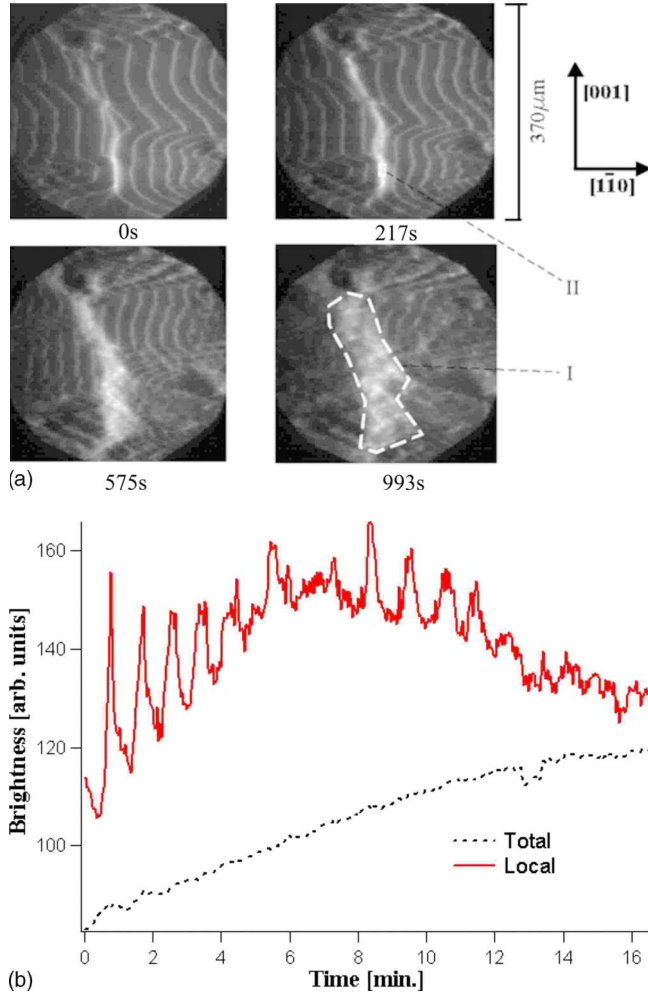


FIG. 1. (Color online) PEEM experiment demonstrating the enrichment of K in the collision area of two pulse trains. (a) PEEM images showing two pulse trains coming from two target patterns centered left and right outside the imaged area. Indicated are the areas in which the intensity has been integrated [see (b)]. (b) Increase of local brightness (window II) and of the brightness integrated over the whole collision area (window I) during the experiment shown in (a). Experimental conditions: $T=510$ K, $p(\text{NO})=1.5 \times 10^{-6}$ mbar, $p(\text{H}_2)=1.2 \times 10^{-5}$ mbar, $\theta_{\text{K}}^{\text{init}}=0.06$. Time $t=0$ s given by first collision of pulses.

deposited K we can roughly estimate that the local K coverage in the central area reaches about 0.12 ML [14,16]. Under our experimental conditions K does not desorb so that K is just redistributed by the pulses keeping the total amount constant.

For the mathematical description we have as a starting point two well-established realistic models which were shown to successfully reproduce (i) chemical wave patterns in the system $\text{Rh}(110)/\text{NO}+\text{H}_2$ and (ii) the stationary patterns in the K promoted system $\text{Rh}(110)/\text{K}/\text{O}_2+\text{H}_2$ [5,11]. Combining these two models into one and adding site-blocking of K diffusion by coadsorbed nitrogen leads to the following set of coupled partial differential equations (PDEs):

$$\frac{\partial \theta_{\text{H}}}{\partial t} = \tilde{k}_1 p_{\text{H}_2} [\max(\theta_{*,1}, 0)]^2 - k_3 (\theta_{\text{H}})^2 - 2k_5 \theta_{\text{H}} \theta_{\text{O}} + D_{\text{H}} \frac{\partial^2 \theta_{\text{H}}}{\partial x^2}, \quad (1)$$

$$\frac{\partial \theta_{\text{N}}}{\partial t} = k_2 p_{\text{NO}} \max(\theta_{*,2}, 0) - k_4 (\theta_{\text{N}})^2 + D_{\text{N}} \frac{\partial^2 \theta_{\text{N}}}{\partial x^2}, \quad (2)$$

$$\frac{\partial \theta_{\text{O}}}{\partial t} = k_2 p_{\text{NO}} \max(\theta_{*,2}, 0) - k_5 \theta_{\text{H}} \theta_{\text{O}} + D_{\text{O}} \frac{\partial^2 \theta_{\text{O}}}{\partial x^2}, \quad (3)$$

$$\frac{\partial \theta_{\text{K}}}{\partial t} = \frac{\partial}{\partial x} \left\{ g(\theta_{\text{N}}) D_{\text{K}} \frac{\partial \theta_{\text{K}}}{\partial x} \right\} - \frac{E_b}{RT} \frac{\partial}{\partial x} \left\{ g(\theta_{\text{N}}) D_{\text{K}} \tilde{\theta}_{\text{K}} (1 - \tilde{\theta}_{\text{K}}) \frac{\partial \theta_{\text{O}}}{\partial x} \right\}, \quad (4)$$

$$\theta_{*,1} = \begin{cases} 1 - \theta_{\text{H}} - \alpha_1 \theta_{\text{N}} - \beta_1 \theta_{\text{O}} & \text{for } \theta_{\text{N}} < 0.5, \\ 1 - \theta_{\text{H}} - (2 - \alpha_1) \theta_{\text{N}} - \frac{2}{3} - \beta_1 \theta_{\text{O}} & \text{for } \theta_{\text{N}} \geq 0.5, \end{cases}$$

$$\theta_{*,2} = 1 - \theta_{\text{H}} - \alpha_2 \theta_{\text{N}} - \beta_2 \theta_{\text{O}}, \quad \tilde{k}_1 = k_1 \exp(-\delta \theta_{\text{K}}),$$

$$k_4 = \nu_4 \exp\left(\frac{-(E_4^0 - \theta_{\text{O}} E_{\text{Rep}})}{RT}\right),$$

$$D_{\text{K}} = D_{\text{K}}^0 \exp\left(\frac{-[E_{\text{K}}' + \theta_{\text{O}}(E_{\text{K}}'' - E_{\text{K}}')]}{RT}\right),$$

$$\tilde{\theta}_{\text{K}} = \frac{\theta_{\text{K}}}{\theta_{\text{K}}^{\text{max}}},$$

$$\theta_{\text{K}}^{\text{max}} = 0.22; \quad g(\theta_{\text{N}}) = \max(1 - \varepsilon \theta_{\text{N}}, 0).$$

The reaction-diffusion (RD) system (I)–(III), without potassium analyzed in Ref. [12], describes the dissociative chemisorption of hydrogen (\tilde{k}_1) and NO (k_2), the desorption of hydrogen (k_3) and nitrogen (k_4), the formation of water where the addition of the first proton has been assumed to be rate-limiting (k_5), and the diffusion of the three adsorbates. Coadsorbed potassium was shown to drastically reduce the reactivity of chemisorbed oxygen toward hydrogen—an effect encoded via an exponential decrease of the hydrogen sticking coefficient with K coverage (\tilde{k}_1 term)[17].

In Eq. (4) representing the transport of potassium the first term stands for Fickian diffusion while the second term—the so-called drift term—describes the transport of potassium in the gradient of the chemical potential given in this case by the oxygen coverage. E_b is the gain in adsorption energy as K migrates from the clean surface to the oxygen covered surface [8,17]. The much smaller mobility of the K atom on the O-covered surface which results from a stronger energetic corrugation is encoded in a linear increase of the activation energy for K diffusion with the oxygen coverage. Assuming pairwise interactions an influence of oxygen on

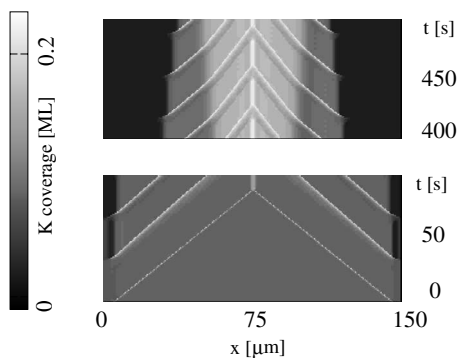


FIG. 2. $x-t$ plots showing in a one-dimensional simulation with Eqs. (1)–(4) the K enrichment in the collision area of two pulse trains. Initial conditions: $\theta_K^{\text{init}}=0.08$, $\theta_H^{\text{init}}=2 \times 10^{-8}$, $\theta_N^{\text{init}}=0.01$, $\theta_O^{\text{init}}=0.89$ except $x < 4 \times 10^{-6}$ m and $x > 1.46 \times 10^{-4}$ m where $\theta_O^{\text{init}}=0.09$. Reaction parameters: $T=550$ K, $p(\text{NO})=1.09 \times 10^{-6}$ mbar, $p(\text{H}_2)=8 \times 10^{-6}$ mbar. T-independent constants: $k_1=2.186 \times 10^6$ ML s $^{-1}$ mbar $^{-1}$; $k_2=1.890 \times 10^5$ ML s $^{-1}$ mbar $^{-1}$; $\alpha_1=5/3$; $\alpha_2=1.05$; $\beta_1=1.1$; $\beta_2=1.115$, $\delta=6$, $\varepsilon=5$, $E_b=15$ kJ mol $^{-1}$. T-dependent constants expressed as $k_i=v_i \exp(-E_i/RT)$; v_i in [s $^{-1}$], E_i in [kJ mol $^{-1}$]: $k_3: 10^{13}$, 72; $k_4: 10^{10}$, $E_4^0=118$, $E_{\text{rep}}=24$; $k_5: 10^{13}$, 90. Diffusion constants as $D_j=D_j^0 \exp(-E_j/RT)$ with D_j^0 in [cm 2 s $^{-1}$], E_j in [kJ mol $^{-1}$]: $D_H: 6.25 \times 10^{-5}$, 18; $D_N: 3.125 \times 10^{-7}$, 40; $D_O: 0.4$, 120; K diffusion: $D_K^0=6.25 \times 10^{-2}$ cm 2 s $^{-1}$, $E'=37.8$ kJ mol $^{-1}$, and $E''=84.8$ kJ mol $^{-1}$.

potassium diffusion automatically implies that coadsorbed potassium also influences oxygen diffusion. A corresponding symmetrical term to the second diffusion term in Eq. (4) should therefore appear in Eq. (3) accounting for the effect of coadsorbed potassium on oxygen diffusion. We have carried out simulations with this additional term but the effect turned out to be very small so that this term can be dropped. The reason for the small effect is that oxygen diffusion at 500–600 K is still very slow. The K-O interaction energy modifies the large energy barrier for oxygen diffusion only slightly, quite in contrast to the very mobile potassium where the same K-O interaction energy has a drastic effect.

Scanning photoelectron microscopy showed that the traveling N-pulses are essentially free of K which prefers to be coadsorbed with oxygen [10]. The energetic driving force for this phase separation is that nitrogen induces a different type of reconstruction than the missing row type which is favorable for adsorbed K [18]. We therefore introduce a site-blocking for diffusing K by N_{ad} the strength of which is controlled by the parameter ε . Nearly all constants could be taken from experiment and only ε had to be treated as a fit parameter. The system of equations (1)–(4) was numerically integrated over a one-dimensional domain of length L applying periodic boundary conditions (PBCs).

With the above system we can reproduce the mass transport of potassium by traveling pulses, or rather pulslike solutions (see below) and the enrichment in the collision area as demonstrated in the simulation results in Figs. 2 and 3. The basic excitation cycle of the unpromoted system is still intact: Reactive removal of the oxygen adlayer by hydrogen leads to a nitrogen covered surface, but as oxygen from dissociatively adsorbing NO displaces the less strongly bonded nitrogen, the initial state of an oxygen covered surface is

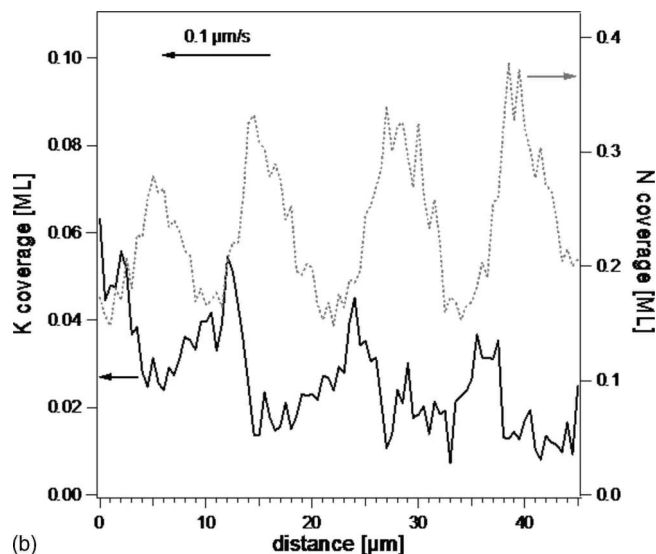
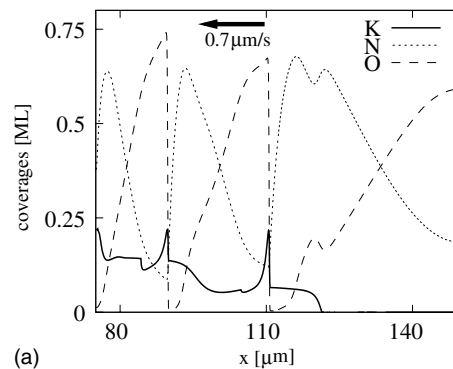


FIG. 3. Comparison of simulated and experimental concentration profile of a pulse. (a) Simulated profile at $t=400$ s. Parameters as in Fig. 2. (b) Concentration profile as determined from XPEEM. The locally measured (spot diameter 2 to 3 μm) XPS intensity of N 1s and K 2p has been converted into a spatial profile assuming a constant pulse velocity of 0.1 $\mu\text{m/s}$ and a constant pulse profile. Both assumptions are only approximately fulfilled. The first few pulses after start of the experiment are not captured. Experimental conditions: $T=469$ K, $p(\text{NO})=2.5 \times 10^{-7}$ mbar, $p(\text{H}_2)=6.7 \times 10^{-7}$ mbar, $\theta_K^{\text{init}}=0.05$, $h\nu=459$ eV.

established again. Since nitrogen acts as a diffusion barrier K is essentially pushed by the nitrogen pulse so that a significant K concentration builds up in front of the pulse. If one neglects site-blocking by nitrogen no K is transported by traveling pulses. This picture is confirmed by micro-XPS measurements as demonstrated by the concentration profile of a propagating pulse in Fig. 3(b). Each pulse carries only a small amount of potassium and θ_K in front of a pulse increases only by about 2% of a ML. The simulation yields about the same amount of transported K with each pulse. In the experiment (Fig. 1) as well as in the simulation (Fig. 2) we see that the collision of a number of pulses is required to build up a substantial K coverage in the collision area. Fast redistribution of the enriched K is prohibited by coadsorbed oxygen which practically immobilizes the potassium.

Under the conditions of Fig. 2, the system shows the interesting property that a steep gradient in the K coverage can

trigger the formation of new pulses. This is exploited in the simulation to let the boundary region periodically emit new pulses after having initiated the very first pulse by putting a hole into the oxygen adlayer. The objects we have so far described as pulses are not perfect homoclinic orbits in domains of finite length, especially when, under K transport conditions, the K levels differ ahead and behind these traveling concentration wave structures; with a slight abuse of nomenclature we will still designate them as pulses. It is therefore crucial that for a given set of $p(\text{NO})$, $p(\text{O}_2)$, $p(\text{H}_2)$, and T reaction conditions the system possesses an entire one-parameter family of pulses, parametrized by the average K coverage. This way the pulses can travel on different K backgrounds, and in particular can travel up a moderate K gradient towards the middle of the domain, which results from earlier collisions of pulses.

More insight into the family of pulses was obtained from a traveling wave stability analysis of the PDE system (1)–(4) [19]. Introducing a comoving frame $y=x-ct$ with c being the pulse velocity, one obtains families of pulses, each characterized by a different average K coverage (and also a different speed). Linearization around the pulses then automatically yields a double zero eigenvalue with one eigenvector being associated with the translational invariance and the other one indicating how the shape of the pulse changes with varying average K coverage.

Continuation with respect to operating parameters (e.g., the temperature, the NO partial pressure) reveals that such stable pulse trains (in finite length domains and with periodic boundary conditions) can lose stability, “splitting” into two different fronts connecting the stable rest state with an unstable fixed point (approaching a double heteroclinic connection); this is a global bifurcation associated with their continuous spectrum. Choosing operating parameters in this unstable pulse train regime, as in Fig. 2, leads in simulations to repeated “firing” from the boundary; over large times this results in substantial K accumulation at the center of the domain.

In summary, for an excitable system we have shown in experiment as well as through modeling that an additional nonreacting species with strong energetic interactions with the reactants can be transported by traveling pulses. The effect could be explained in terms of a detailed microscopic picture. One should expect that this effect will be found in a number of surface reactions, as well as in other systems with similar energetic interactions. The resulting enrichment of a species introduces a memory effect into a system and thus might serve as a building block for more complex dynamics.

The work of I.G.K. was partially supported by DARPA and AFOSR.

-
- [1] *Chemical Waves and Patterns*, edited by R. Kapral and K. Showalter (Kluwer, Dordrecht, 1994).
- [2] J. Verdasca, P. Borckmans, and G. Dewel, *Phys. Rev. E* **52**, R4616 (1995).
- [3] M. Hildebrand, A. S. Mikhailov, and G. Ertl, *Phys. Rev. Lett.* **81**, 2602 (1998).
- [4] Y. D. Decker, H. Marbach, M. Hinz, S. Günther, M. Kiskinova, A. S. Mikhailov, and R. Imbihl, *Phys. Rev. Lett.* **92**, 198305 (2004); Y. De Decker and A. S. Mikhailov, *J. Phys. Chem. B* **108**, 14759 (2004).
- [5] S. C. Glotzer, E. A. Di Marzio, and M. Muthukumar, *Phys. Rev. Lett.* **74**, 2034 (1995).
- [6] Y. Tabe and H. Yokoyama, *Langmuir* **11**, 4609 (1995).
- [7] H. Marbach *et al.*, *Catal. Lett.* **83**, 161 (2002); M. Hinz, S. Günther, H. Marbach, and R. Imbihl, *J. Phys. Chem. B* **108**, 14620 (2004).
- [8] A. Locatelli *et al.*, *J. Phys. Chem. B* **110**, 19108 (2006).
- [9] V. P. Zhdanov, *Phys. Chem. Chem. Phys.* **7**, 2399 (2005).
- [10] H. Marbach, S. Günther, T. Neubrand, and R. Imbihl, *Chem. Phys. Lett.* **395**, 64 (2004).
- [11] F. Mertens and R. Imbihl, *Nature (London)* **370**, 124 (1994); N. Gottschalk, F. Mertens, M. Bar, M. Eiswirth, and R. Imbihl, *Phys. Rev. Lett.* **73**, 3483 (1994).
- [12] A. Makeev, M. Hinz, and R. Imbihl, *J. Chem. Phys.* **114**, 9083 (2001).
- [13] Th. Schmidt *et al.*, *Surf. Rev. Lett.* **5**, 1287 (1998).
- [14] S. Günther *et al.*, *J. Chem. Phys.* **124**, 014706 (2006).
- [15] M. Kiskinova, *Stud. Surf. Sci. Catal.* **70**, 30 (1992).
- [16] This value probably represents a lower limit for θ_K^{max} because the coadsorption with oxygen will lower the WF in the collision area.
- [17] S. Günther *et al.*, *J. Chem. Phys.* **119**, 12503 (2003).
- [18] M. Kiskinova, *Chem. Rev. (Washington, D.C.)* **96**, 1431 (1996).
- [19] L. Qiao *et al.*, (unpublished).